Critical membrane concentration and mass-balance model to identify baseline cytotoxicity of hydrophobic and ionizable organic chemicals in mammalian cell lines

Jungeun Lee,[†] Georg Braun,[†] Luise Henneberger,[†] Maria König,[†] Rita Schlichting[†], Stefan Scholz,[§] Beate I. Escher,[†‡]*

[†]Department of Cell Toxicology, Helmholtz Centre for Environmental Research – UFZ, Permoserstr. 15, DE-04318 Leipzig, Germany,

[§]Department of Bioanalytical Toxicology, Helmholtz Centre for Environmental Research – UFZ, Permoserstr. 15, DE-04318 Leipzig, Germany,

[‡]Environmental Toxicology, Center for Applied Geoscience, Eberhard Karls University Tübingen, Schnarrenbergstr. 94-96, DE-72076 Tübingen, Germany

*Address correspondence to: beate.escher@ufz.de

Key words

Cell-based bioassays, reporter gene assays, high-throughput screening, narcosis, quantitative structure-activity relationship, QSAR

Table of Contents (TOC) graphic

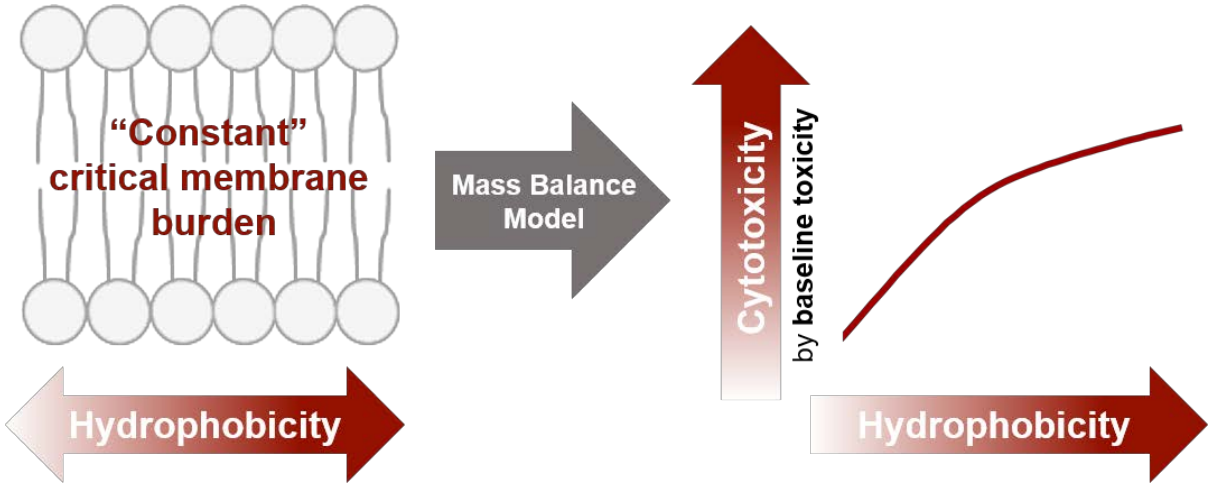

ABSTRACT

All chemicals can interfere with cellular membranes and this leads to baseline toxicity, which is the minimal toxicity any chemical elicits. The critical membrane burden is constant for all chemicals, that is, the dosing concentrations to trigger baseline toxicity decrease with increasing hydrophobicity of the chemicals. Quantitative structure-activity relationships—based on hydrophobicity of chemicals—have been established to predict nominal concentrations causing baseline toxicity in human and mammalian cell lines. However, their applicability is limited to hydrophilic neutral compounds. To develop a prediction model that includes more hydrophobic and charged organic chemicals, a mass balance model was applied for mammalian cells (AREc32, AhR-CALUX, PPARγ-BLA, and SH-SY5Y) considering different bioassay conditions. The critical membrane burden for baseline toxicity was converted into nominal concentration causing 10% cytotoxicity by baseline toxicity ($IC_{10,baseline}$) using a mass balance model whose main chemical input parameter was the liposome-water partition constants ($K_{lip/w}$) for neutral chemicals or the speciation-corrected $D_{lip/w}$(pH 7.4) for ionizable chemicals plus the bioassay-specific protein, lipid, and water contents of cells and media. In these bioassay-specific models, $\log(1/IC_{10,baseline})$ increased with increasing hydrophobicity and the relationship started to level off at $\log D_{lip/w}$ around 2. The bioassay-specific models were applied to 392 chemicals covering a broad range of hydrophobicity and speciation. Comparing the predicted $IC_{10,baseline}$ and experimental cytotoxicity

IC_{10}, known baseline toxicants and many additional chemicals were identified as baseline toxicants, while the others were classified based on specificity of their modes of action in the four cell lines, confirming excess toxicity of some fungicides, antibiotics, and uncouplers. Given the similarity of the bioassay-specific models, we propose a generalized baseline-model for adherent human cell lines: $\log(1/IC_{10,baseline}(M))=1.23+4.97\times\left(1-e^{-0.236\log D_{lip/w}}\right)$. The derived models for baseline toxicity may serve for specificity analysis in reporter gene and neurotoxicity assays as well as for planning the dosing for cell-based assays.

INTRODUCTION

Modes of action (MOA) describe how toxic chemicals act on their target, and can be classified into baseline, reactive, and specific toxicity.[1, 2] Principally, all chemicals cause baseline toxicity because it is their minimal toxicity caused by the interference of the chemicals with the membrane. Chemicals with more specific MOAs exhibit toxic effects before the baseline toxicity occurs. Therefore, we can identify whether chemicals act through baseline toxicity or more specific MOA by comparing expected baseline toxicity level and the observed toxicity, and the ratio between these two toxicity levels is defined as toxic ratio (TR), which is an indicator for specificity of MOA.[1, 3]

Quantitative structure-activity relationships (QSARs) for baseline toxicity describe the relationship between nominal effect concentrations for baseline toxicity and liposome-water partition constants ($K_{lip/w}$), a proxy for biomembrane-water partition constants. Nominal effect concentrations for baseline toxicity depend on hydrophobicity of chemicals. Hydrophobic chemicals can exhibit baseline toxicity at lower nominal concentrations than hydrophilic chemicals as they will accumulate better in cell membranes than hydrophilic chemicals. The QSARs have been established experimentally from effect concentrations of confirmed baseline toxicants in aquatic animals,[4-6] and even extended to ionizable organic compounds (IOCs).[7, 8] QSAR equations for baseline toxicity have also been developed for eight reporter gene cell lines derived from human and animal cells.[9] The existing QSARs for *in vitro* assays were based on hydrophilic and neutral compounds ($0.5 < \log K_{lip/w} < 4.5$), which limits their application to more hydrophobic and charged organic chemicals.

Mass balance models (MBM) can convert nominal concentration (C_{nom}) into membrane concentration (C_{mem}) or freely dissolved concentration (C_{free}) at equilibrium, or *vice versa*, by considering chemical partitioning between different compartments of the bioassay system. C_{nom} is widely used as a dose metric in *in vitro* assays, but bioavailable portion even from the same C_{nom} may vary for a given chemical depending on the bioassay system. This variability is believed to result mainly from sorption of the chemicals to the biomolecules in the medium such as proteins and lipids, which reduces bioavailability and uptake into cells. Alternatively, C_{mem} and C_{free} have been suggested as more accurate

dose metrics than C_{nom} because they better reflect bioavailable concentration and interaction at the target sites, respectively.[10, 11] C_{mem} leading to baseline toxicity in cell lines, that is, critical membrane burden (CMB) for 10% reduced cell viability, was found to be constant at 69 $mmol \cdot L_{lip}^{-1}$ (95% CI: 49-89) in 8 reporter gene cell lines.[9] The CMB is independent of the type and hydrophobicity of the chemicals[12] including neutral and charged chemicals,[7, 8, 13] and is very similar across different cell types[9, 13] and various aquatic species.[12, 14]

The mass balance models published by Armitage et al.[15] and Fischer et al.[10] described *in vitro* exposure based on chemical partitioning in medium and cells. Each compartment was composed of proteins, lipids, and water, and bovine serum albumin (BSA) and phospholipids represented proteins and lipids in the system, respectively. This model is applicable for both neutral and ionizable compounds, however, the complex behavior of anionic compounds such as specific binding to BSA cannot be modeled simply based on this partitioning process.[16, 17] This particularly matters for organic acids that are predominantly negatively charged at the pH 7.4 of the medium.

The aim of this study was to develop a model to predict baseline toxicity, which has a broad applicability in terms of hydrophobicity and speciation (Figure 1). Instead of trying to expand the existing baseline QSAR developed based on hydrophilic known baseline toxicants, we propose a bioassay-specific MBM to predict the nominal inhibitory concentration for cytotoxicity (IC_{10}) from the constant CMB (Figure 1). The predicted nominal baseline toxicity $IC_{10,baseline}$ can then be compared with experimental IC_{10} to identify chemicals that act as baseline cytotoxicants in mammalian cell lines. Our workflow includes evaluation, simplification, and application of the model as outlined in Figure S1. 253 neutral and 139 ionizable compounds were included, which cover broad ranges of hydrophobicity, speciation, and MOA. Four mammalian cell lines were applied to simulate diverse scenarios with different composition of cells and medium. First, the predicted relationship between partition constants, which is premise of our model, was verified by experimental partition constants. The MBM was then used to predict $IC_{10,baseline}$ solely based on $K_{lip/w}$, and was applied initially to compounds with experimental partition constants. Lastly, the developed model was simplified for ease of application, and TR was derived from $IC_{10,baseline}$ and experimental IC_{10} to identify baseline toxicants in the test set of chemicals with experimental data.

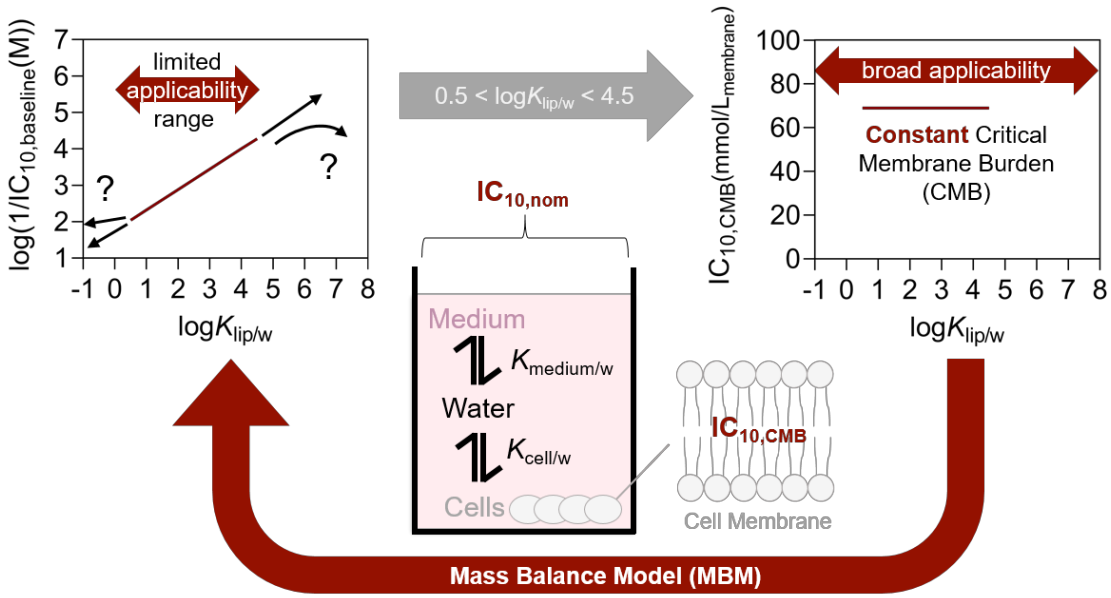

Figure 1. Outline of the study. Chemical distribution between medium, water, and cells was described by $K_{medium/w}$ and $K_{cell/w}$ in a mass balance model (MBM). Nominal concentration causing 10% cytotoxicity by baseline toxicity ($IC_{10,baseline}$) was predicted from critical membrane burden (CMB) for 10% reduced cell viability ($IC_{10,CMB}$) through MBM, and the predicted $IC_{10,baseline}$ was compared with nominal concentration for 10% cytotoxicity from experiment ($IC_{10,nom}$).

THEORY

Mass balance model for baseline toxicity

The mass balance model outlined in Figure 1 is a nested model with just two boxes, one for medium and one for cells.[10] Each box is made up of water, proteins, and lipids, albeit with different composition. Water from medium connects cells and the other components of medium, and mediates the partitioning processes between the two boxes. The partitioning between medium and cells ($K_{medium/cell}$) can be broken up into two partitioning processes, the partitioning between medium and water described by the medium-water partition constant ($K_{medium/w}$) and the partitioning between cells and water described by the cell-water partition constant ($K_{cell/w}$).

Within medium and cells, the chemicals can partition between three compartments, i.e., proteins, lipids, and water, and therefore the $K_{medium/w}$ can be described by the partition constants between proteins and water ($K_{protein/w}$) and the volume fraction of proteins ($Vf_{protein,medium}=V_{protein,medium}/V_{medium}$), the partition constants between lipids and water ($K_{lip/w}$) and the volume fraction of lipids ($Vf_{lip,medium}=V_{lip,medium}/V_{medium}$), as well as the volume fraction of water ($Vf_{w,medium}=V_{w,medium}/V_{medium}$) (eq. 1).[10] The analogous equation is defined for $K_{cell/w}$ (eq. 2).[10]

$$K_{medium/w} = Vf_{protein,medium} \cdot K_{protein/w} + Vf_{lip,medium} \cdot K_{lip/w} + Vf_{w,medium} \quad (1)$$

$$K_{cell/w} = Vf_{protein,cell} \cdot K_{protein/w} + Vf_{lip,cell} \cdot K_{lip/w} + Vf_{w,cell} \quad (2)$$

Applying a mass balance we can then calculate the fraction of chemicals in medium (f_{medium}, eq. 3) and cells (f_{cell}, eq. 4).[10]

$$f_{medium} = \frac{1}{1 + \frac{K_{cell/w} V_{cell}}{K_{medium/w} V_{medium}}} \quad (3)$$

$$f_{cell} = \frac{1}{1 + \frac{K_{medium/w} V_{medium}}{K_{cell/w} V_{cell}}} \quad (4)$$

The mass balance model inside the cell[9] connects the membrane concentration in the cell ($C_{membrane}$ in general or specifically for the concentration causing 10% cytotoxicity $IC_{10,membrane}$) to the total cellular concentration (C_{cell} or $IC_{10,cell}$) by eq. 5 with $f_{lip,cell}$ (eq. 6) being the fraction of chemical in the lipids of the cell. The $IC_{10,cell}$ can then be converted to nominal concentrations that lead to 10% cytotoxicity, IC_{10} by eq. 7.

$$IC_{10,cell} = IC_{10,membrane} \cdot \frac{Vf_{lip,cell}}{f_{lip,cell}} \quad (5)$$

$$f_{lip,cell} = \frac{1}{1 + \frac{1}{K_{lip/w} V_{lip,cell}} V_{w,cell} + \frac{K_{protein/w} V_{protein,cell}}{K_{lip/w} V_{lip,cell}}} \quad (6)$$

$$IC_{10} = \frac{IC_{10,cell}}{f_{cell}} \cdot \frac{V_{cell}}{V_{medium} + V_{cell}} \quad (7)$$

The critical membrane concentration for baseline toxicity (CMB) corresponds to an $IC_{10,membrane}$ of 69 mM.[9] The associated nominal $IC_{10,baseline}$ for baseline toxicity can be calculated by combining eqs. 4, 5, and 7.

$$IC_{10,baseline}(M) = 0.69 \cdot \frac{Vf_{lip,cell}}{f_{lip,cell}} \cdot \frac{V_{cell}}{V_{medium} + V_{cell}} \cdot \left(1 + \frac{K_{medium/w}}{K_{cell/w}} \cdot \frac{V_{medium}}{V_{cell}}\right) \quad (8)$$

Since $V_{medium} >> V_{cell}$, we can simplify eq. 8 to yield eq. 9.

$$IC_{10,baseline}(M) = 0.69 \cdot \frac{Vf_{lip,cell}}{f_{lip,cell}} \cdot \left(\frac{V_{cell}}{V_{medium} + V_{cell}} + \frac{K_{medium/w}}{K_{cell/w}}\right) \quad (9)$$

$K_{lip/w}$ as a sole descriptor of the mass balance model

In cells, the $K_{protein/w}$ of neutral chemicals can be approximated with BSA as protein surrogate ($K_{BSA/w}$). The liposome-water partition constant ($K_{lip/w}$) uses liposomes as surrogate for the cell lipids, which are mainly membrane lipids.

$K_{BSA/w}$ and $K_{lip/w}$ of neutral organic chemicals can be predicted by simple QSARs from the octanol-water partition constant ($\log K_{ow}$).[18, 19]

$$\log K_{BSA/w} = 0.71 \cdot \log K_{ow} + 0.42 \qquad (n = 76,\ R^2 = 0.76,\ SD = 0.43) \qquad (10)$$

$$\log K_{lip/w} = 1.01 \cdot \log K_{ow} + 0.12 \qquad (n = 156,\ R^2 = 0.948,\ SD = 0.426) \qquad (11)$$

The QSAR for $K_{BSA/w}$ was linear for $1 < \log K_{ow} < 7$,[19] which agreed with the earlier observation that there was approximately a factor of 20 between $K_{BSA/w}$ and $K_{lip/w}$ for neutral chemicals down to $\log K_{ow}$ of 2, below which the $K_{BSA/w}$ was levelling off to 1.31±0.62.[20]

The QSAR for $K_{lip/w}$ was linear for $-1 < \log K_{ow} < 8$[18] and stayed virtually constant at a $\log K_{lip/w}$ of -1 for $\log K_{ow} < -1$.[21]

If eqs. 10 and 11 were combined, a direct linear relationship between $K_{lip/w}$ and $K_{BSA/w}$ was obtained (K_{ow} QSAR, eq. 12).

$$\log K_{BSA/w} = 0.72 \cdot \log K_{lip/w} + 0.34 \qquad (12)$$

This means that the $IC_{10,baseline}$ can be predicted for chemicals, for which eq. 12 holds, merely from the $\log K_{lip/w}$ and lipid and protein content of cells and medium. Therefore, this model is theoretically valid only for neutral chemicals. After implementing the model with experimental data for neutral chemicals, we attempt to extend it also to charged chemicals. There are more sophisticated models based on linear solvation energy relationships (LSER), which have been used to retrieve physicochemical properties for the model evaluation, but the baseline toxicity prediction model was meant to be as simple as possible and based on as few input parameters as possible. The $\log K_{lip/w}$ can even be substituted by the readily available $\log K_{ow}$ (eq. 11).

MATERIALS AND METHODS

Chemicals and partition constants. 392 chemicals were included in the present analysis (Table S1). All chemicals are listed together with their name, DTXSID, CAS number and physicochemical properties in Table S2. Experimental octanol-water partition constant $\log K_{ow}$ stemmed mainly from PhysPropNCCT or were predicted with using the OPERA model and both were retrieved from the US EPA Comptox Chemistry Dashboard.[22]. The acidity constant pK_a and the fraction of neutral and charged species were predicted with ACD/Percepta.[23]

For liposome-water partitioning of the neutral species $K_{lip/w}$, experimental values [7, 18, 24-31] were preferred over predictions by Linear Solvation Energy Relationships (LSER).[32] If no experimental LSER descriptors were available, the $K_{lip/w}$ was predicted from K_{ow} with eq. 11 (Table S2). If logK_{ow} < -1, $K_{lip/w}$ was fixed at -1.[21] For IOCs with one charged species, the distribution ratio $D_{lip/w}$(pH 7.4) considered their speciation, and experimental values were used, if available,[7, 8, 16-18, 24, 26, 27, 33-35] or calculated from experimental data of the pure species (a few predicted by COSMOmic[8, 33]) and the fraction of neutral species ($\alpha_{neutral}$) with eq. 13. For the chemicals with multiple charged species, $D_{lip/w}$(pH 7.4) was measured directly at pH 7.4.[16, 17, 34] If only the $K_{lip/w}$ of the neutral species was available, the $K_{lip/w}$ of the charged species was assumed to be 10 times lower (Δmw = 1) and $D_{lip/w}$(pH 7.4) was calculated with eq. 14.[36]

$$D_{lip/w}(\text{pH 7.4}) = \alpha_{neutral} \times K_{lip/w}(\text{neutral species}) + (1-\alpha_{neutral}) \times K_{lip/w}(\text{charged species}) \quad (13)$$

$$D_{lip/w}(\text{pH 7.4}) = K_{lip/w}(\text{neutral species}) \left[\alpha_{neutral} + 10^{-\Delta mw}(1 - \alpha_{neutral})\right] \quad (14)$$

The binding to proteins was approximated by $K_{BSA/w}$, and only experimental values directly measured at pH 7.4[16-18, 37-39] were used for evaluation of the model. For organic acids, BSA is not a suitable model for cellular proteins and therefore experimental distribution ratios to structural proteins ($D_{SP/w}$) as well as experimental distribution ratios between medium and water ($D_{medium/w}$) and cells and water ($D_{cell/w}$) were also retrieved from literature[16, 40] and are listed in Table S3.

Experimental partition constants for, both, lipids and proteins, were available for less than 10% of the chemicals (Table S1) and, therefore, the mass balance model was initially applied only for these chemicals that had both types of experimental data to judge its applicability. After it was established that the model produced reasonable predictions, it was applied to all chemicals that had experimental (23% of the neutral chemicals and 29% of the IOCs) or predicted partition constant for lipids (Table S1).

Cell lines. Three reporter gene cell lines (AREc32, AhR-CALUX, and PPARγ-BLA) and a human neuroblastoma cell line SH-SY5Y were applied in this study (Table 1). The cell lines were obtained from different sources – AREc32 by courtesy of C. Roland Wolf (Cancer research UK), AhR-CALUX (H4L7.5c2) by courtesy of Michael Denison (UC Davis, USA), PPARγ-BLA from Thermo Fisher Scientific (Schwerte, Germany), and SH-SY5Y from Sigma-Aldrich. SH-SY5Y were differentiated with 10 µM of all-trans retinoic acid (Sigma-Aldrich, R2625) for 72 h before plating. The focus of the study was cytotoxicity and only cytotoxicity was discussed for these four cell lines. For the newly measured hydrophobic compounds (Table S4), the reporter gene activation was additionally reported for the sake of completion. The total volume of the cells (V_{cell}) and their Vf of water, proteins and lipids were previously quantified or newly calculated for the reporter gene cell lines,[9] and measured for differentiated SH-SY5Y cells using the reported methods[10] (Table 1).

Table 1. Reporter Gene Cell Lines Evaluated and Descriptors for the Mass Balance Models Taken from Our Previous Study[9] and Determined Newly for SH-SY5Y. Reprinted (Adapted) with Permission from Escher, B.I., Glauch, L., Konig, M., Mayer, P. and Schlichting, R. (2019). Baseline Toxicity and Volatility Cutoff in Reporter Gene Assays Used for High-Throughput Screening. Chemical Research In Toxicology, 32(8): 1646-1655. Copyright (2019) American Chemical Society.

Cell lines	Derived from	Number of plated cells/well[a]	Mean cell number in assay[b]	Total volume of cells V_{cell} (nL)	$Vf_{water,cell}$ (mL/L)	$Vf_{protein,cell}$ (mL/L)	$Vf_{lip,cell}$ (mL/L)
AREc32	MCF7	2500	4300±290	43.0	944[c]	51[c]	5[c]
AhR-CALUX	H4IIe	3000-3250	5360±750	18.9	939[c]	55[c]	6[c]
PPARγ-BLA	HEK293H	4500-5500	5940±760	17.1	887[d]	80[d]	34[d]
SH-SY5Y	SH-SY5Y	3000	3280±20	6.43	942[e]	47[e]	10[e]

[a] The total volume of medium was 40 µL medium per well in 384-well plates; [b]Cell number is an average between plated cells and final cell number after 24 h of exposure; [c]Henneberger et al;[16] [d]Fischer et al.;[10] [e]this study.

Assay medium. The medium for AREc32 and AhR-CALUX is DMEM GlutaMAX supplemented with 10% FBS and has a protein content $Vf_{protein,medium}$ of 8.93 mL/L and a lipid content $Vf_{lip,medium}$ of 0.14 mL/L.[16] PPARγ-BLA is grown in OptiMEM supplemented with 2% cs-FBS with $Vf_{protein,medium}$ of 4.84 mL/L and a lipid content $Vf_{lip,medium}$ of 0.02 mL/L.[16] The Neurobasal medium (w/o phenol-red) for SH-SY5Y was composed of 2% B-27 Supplement, 2% GlutaMAX Supplement and was newly characterized with the methods published previously[10] resulting in a $Vf_{protein,medium}$ of 2.58 mL/L and a negligible $Vf_{lip,medium}$. All medium contained 100 U/ml Penicillin and 100 µg/mL Streptomycin and all medium constituents were purchased from Thermo Fisher Scientific.

Plating. The cells were plated using a MultiFlo Dispenser (Biotek, Vermont, USA) in 384-well plates and incubated for 24 h at 37 °C and 5% CO_2. The number of cells plated is shown in Table 1. The plates were TC-treated for AREc32, Poly-D-Lysine-coated for AhR-CALUX and PPARγ-BLA, and collagen I–coated plates for SH-SY5Y, and all plates were purchased from Corning (Maine, USA).

Dosing and cytotoxicity measurements. For the reporter gene cell lines, chemical stocks dissolved in DMSO were dosed using a Tecan D300e Digital Dispenser (Tecan, Crailsheim, Germany) as described previously, and cell confluency was quantified before dosing and after 24h of exposure using an IncuCyte S3 live cell imaging system (Essen BioScience, Ann Arbor, Michigan, USA). For SH-SY5Y, chemical stocks were prepared in MeOH due to their high sensitivity to DMSO. The stocks were added into the assay medium, and the dosing medium was diluted and dosed using a pipetting robot (Hamilton

Star, Bonaduz, Switzerland). After 24 h exposure, Nuclear Green LCS1 (Abcam, ab138904) and propidium iodide (Sigma-Aldrich, 81845) were added to stain total and dead cells at final concentrations in the well plates of 10 µM and 1 µM, respectively. The cells were stained for 1 h in incubator, and cell viability was derived by image analysis with the IncuCyte S3.

Cytotoxicity was expressed as % inhibition of cell viability (% cytotoxicity) relative to unexposed cells from measurements of confluency for reporter gene cell lines as described in detail previously.[9] For SH-SY5Y cells, cell viability was calculated based on the ratio of live cell count to total cell count and its relative inhibition to unexposed cells was determined as % cytotoxicity. The concentration causing 10% cytotoxicity (IC_{10}, eq. 16) was derived from the slope of the linear portion of the concentration response curve (eq. 15), which was typically linear up to 30 to 40% effect.[41]

$$\%\ \text{cytotoxicity} = \text{slope} \times \text{concentration} \tag{15}$$

$$IC_{10} = \frac{10\%}{\text{slope}} \tag{16}$$

The majority of IC_{10} values listed in Table S2 was already published earlier[9, 42-46] but to expand the MBM also to more hydrophobic chemicals, we measured additional 75 hydrophobic neutral chemicals in AREc32, AhR-CALUX, and PPARγ-BLA and the resulting IC_{10} values are given in Table S4. For SH-SY5Y, cytotoxicity was determined within this study and the resulting IC_{10} values are listed in Table S2. Of the total of 392 chemicals included, 271 of 381 tested chemicals had experimental IC_{10} values in AREc32, 271 of 379 tested chemicals in AhR-CALUX, 216 of 370 tested in PPARγ-BLA, and 22 of 48 in SH-SY5Y. The ones tested but without reported IC_{10} values were either tested at concentrations that were too low (Tox21 data were dosed only up to 100 µM and were reevaluated in our previous study with stricter quality control[44]) or precipitated in the assay and thus could not be used. If precipitation occurred in the newly measured chemicals, which was the case for 17 experiments for reporter gene cell lines, this observation was noted in Table S4. In case of SH-SY5Y, hydrophobic chemicals had limited solubility from low content of proteins and lipids in the medium, and therefore precipitates were allowed up to the level where turbidity started to appear. This observation was reported also in Table S4 and these chemicals with precipitate issue can have uncertainty in the determined IC_{10} values.

Toxic ratio. The ratio between the predicted IC_{10} for baseline toxicity ($IC_{10,baseline}$) and the experimental IC_{10} is called the toxic ratio (TR, eq. 17).[1] Chemicals with $TR < 10$ are baseline toxicants and $TR \geq 10$ points to an enhanced toxicity due to a specific mode of action or reactive toxicity.[3]

$$TR = \frac{IC_{10,baseline}}{IC_{10}} \tag{17}$$

RESULTS AND DISCUSSION

Distribution ratios. The mass balance model for baseline toxicity relies on a predictable relationship between liposome-water partitioning and protein-water partitioning. This relationship was derived from published QSARs and resulted in a linear QSAR equation between $K_{lip/w}$ and $K_{BSA/w}$ (eq. 12, red line in Figure 2A). For 18 neutral chemicals with cytotoxicity data, both experimental $K_{BSA/w}$ and $K_{lip/w}$ were available and corresponded remarkably well with the QSAR (Figure 2A; mean absolute percentage error (MAPE): 12.7%). For very hydrophobic neutral chemicals, the $K_{lip/w}$ was approximately 20 times higher than the $K_{BSA/w}$, as already reported by DeBruyn and Gobas,[20] but at lower hydrophobicity the values came closer to each other. At low hydrophobicity ($\log K_{ow} < 2$), the $K_{BSA/w}$ was reported to be 1.31 on average and independent of the hydrophobicity.[20]

For IOCs, their speciation at pH 7.4 should be considered to derive distribution ratios between BSA and water ($D_{BSA/w}$) and between liposomes and water ($D_{lip/w}$). Both experimental distribution ratios $D_{BSA/w}$(pH 7.4) and $D_{lip/w}$(pH 7.4) were available for 12 acids, 5 bases, and 3 multiprotic compounds. Bases and multiprotic chemicals fell well into the prediction range of the QSAR (Figure 2B; MAPE for bases: 25.1%; MAPE for multiprotic chemicals: 26.1%), which is consistent with earlier observations that simple mass balance models can be applied for these types of IOCs.

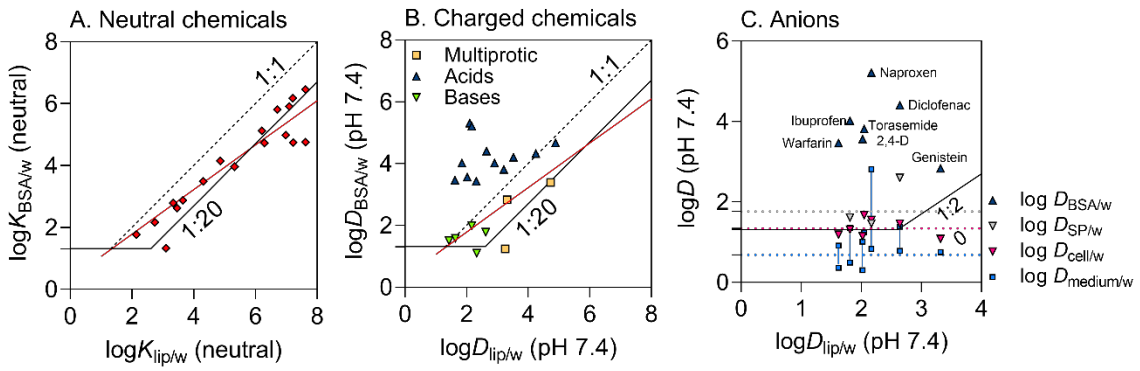

Figure 2. Relationship between liposome-water partitioning ($K_{lip/w}$) and protein (BSA)-water partitioning ($K_{BSA/w}$) of (A) 18 neutral chemicals and (B) ionizable organic chemicals (IOCs; 12 acids, 5 bases and 3 multiprotic compounds). Data from Table S2. The red line in both plots is the $K_{BSA/w}$–$K_{lip/w}$ QSAR (eq. 12) and does not constitute a regression of the experimental data. The black line is the 1:20 line reported to be the approximate relationship by DeBruyn and Gobas,[20] which levels off to a constant value of average log $K_{BSA/w}$ of 1.31 at low logK_{ow}. (C) Comparison of $D_{lip/w}$(pH 7.4) (L_w/L_{lip}) with various distribution ratios D, including binding to BSA ($D_{BSA/w}$(pH 7.4) (L_w/L_{BSA})),[38] structural proteins ($D_{SP/w}$(pH 7.4) (L_w/kg_{SP})),[40, 47] and distribution between cells and water ($D_{cell/w}$(pH 7.4) (L_w/L_{cell})) and medium and water ($D_{medium/w}$(pH 7.4) (L_w/L_{medium})). Range (blue lines) are given for $D_{medium/w}$ because of nonlinear binding isotherms.[35] The dotted lines represent the mean of the depicted log$D_{SP/w}$, log$D_{cell/w}$, and log$D_{medium/w}$, and the lower value at saturated binding for medium. Data from Table S3.

However, organic acids showed much stronger binding to BSA than predicted from partitioning to lipids (Figure 2B; MAPE: 43.6%). To explore the relationship between $D_{BSA/w}$(pH 7.4) and $D_{lip/w}$(pH 7.4) for organic acids more clearly, we evaluated more organic acids, for which no cytotoxicity data were available, but no clearer pattern emerged (Figure S2)—the perfluoroalkyl substances having a ratio of $D_{BSA/w}$(pH 7.4)/$D_{lip/w}$(pH 7.4) of 10 to 1, the carboxylic acids even higher, and the two substituted phenols divergent (10 and 1000). These divergent ratios confirm that binding of anions to BSA cannot be described as a partitioning process. In addition, one needs to consider specific binding to high-affinity sites on BSA that depends on the three dimensional structure of the molecule and the location of the charge.[38] This specific binding is saturable, which makes binding of anions to BSA concentration-dependent.[16] Therefore, there does not exist a simple relationship between $D_{BSA/w}$(pH 7.4) and $D_{lip/w}$(pH 7.4) for organic anions. The distribution ratios between structural proteins (SP) and water $D_{SP/w}$(pH 7.4) described the binding to cell proteins much better than BSA for organic acids,[16] and their experimental $D_{SP/w}$(pH 7.4) were much smaller than $D_{BSA/w}$(pH 7.4) (Figure 2C, Table S3).

Instead of considering specific types of proteins and lipids as surrogates for proteins and lipids in medium and cells, the experimental distribution ratios between cells and water ($D_{cell/w}$) and medium and water ($D_{medium/w}$) were explored as alternative descriptors for organic acids (Figure 2C, Table S3). Text S1 discusses some options how to develop models for anions (Figure S3) but more experimental data would be required for developing a reliable prediction model for organic anions.

Mass balance model to predict nominal baseline toxicity. As we concluded in theoretical section, $IC_{10,baseline}$ can be predicted merely from the log$K_{lip/w}$ and lipid and protein content of cells and medium for chemicals, for which eq. 12 holds. For each cell line, the lipid and protein content of cells (Table 1) and medium (M&M) is known. Therefore, we simulated $IC_{10,baseline}$ (eq. 9) with the MBM by assuming that eq. 12 is satisfied. In this case, the predicted $IC_{10,baseline}$ (eq. 9) only depends on log$K_{lip/w}$ (Figure 3A).

Log(1/$IC_{10,baseline}$) initially increased linearly with increase of hydrophobicity with a slope of 1 and there was no difference in the $IC_{10,baseline}$ for the different cell lines (Figure 3A). The relationship started to level off at log$K_{lip/w}$ 2, and the flattening of the curve was most pronounced for the assays with highest protein content in the medium (AREc32 and AhR-CALUX supplemented with 10% FBS). PPARγ-BLA, whose medium is only supplemented with 1% FBS, shows lower $IC_{10,baseline}$ and the SH-SY5Y have the highest sensitivity due to the low protein content and negligible lipid content of their medium (Figure 3A). The difference in predicted $IC_{10,baseline}$ was largest between AREc32 and SH-SY5Y leading to 9-fold difference at log$K_{lip/w}$ of 8.

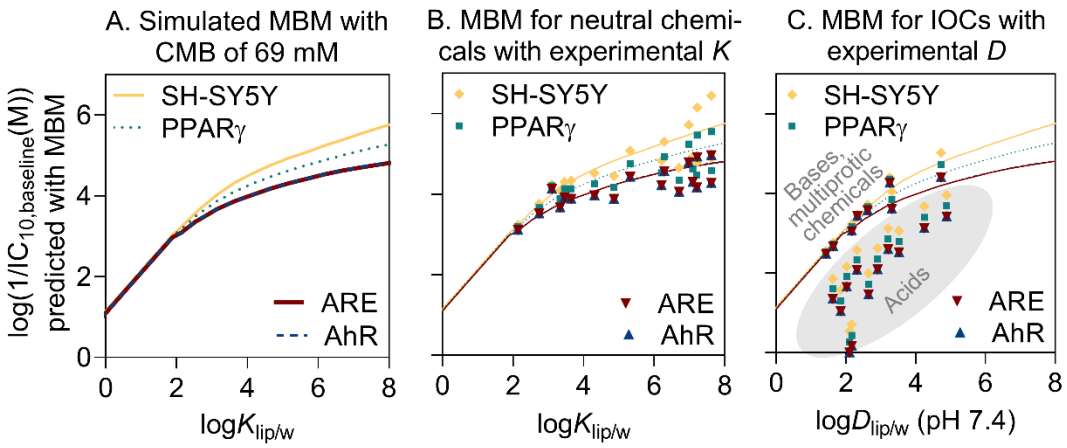

Figure 3. (A) Simulation of $IC_{10,baseline}$ (eq. 9) as a function of $logK_{lip/w}$ using the mass balance model (MBM) with CMB of 69 mM and $K_{BSA/w}$–$K_{lip/w}$ QSAR (eq. 12) to obtain $logK_{BSA/w}$. (B) Evaluation of the simulated MBM (A) with predicted $IC_{10,baseline}$ (symbols) using experimental $K_{lip/w}$ and $K_{BSA/w}$ with the MBM for neutral chemicals. (C) Evaluation of the simulated MBM (A) with predicted $IC_{10,baseline}$ (symbols) using experimental $D_{lip/w}$(pH 7.4) and $D_{BSA/w}$(pH 7.4) with the MBM for IOCs.

The previously published baseline toxicity QSARs[9] were linear but can be interpolated only for 0.5 < log $K_{lip/w}$ < 4.5. The previous QSAR with their slopes of 0.56-0.73 overlays the MBM in this range rather well (Figure S4), confirming the validity of the earlier QSAR. The comparison in Figure S4 demonstrates that the QSAR cannot be linearly extended in either direction because the slope of the linear range of the MBM at log $K_{lip/w}$ < 2 is higher than that of the QSAR equation and there is further flattening at log $K_{lip/w}$ > 4.5.

The simulated MBM built on the linear relationship of $K_{BSA/w}$ and $K_{lip/w}$ (eq. 12) was then compared with $IC_{10,baseline}$ predicted from experimental $K_{BSA/w}$ and $K_{lip/w}$. For neutral compounds, the predictions from experimental values were consistent with the simulated MBM (Figure 3B; MAPE ranges in 4 cell lines between 5.8-7.1%), apart from the three very hydrophobic polycyclic aromatic hydrocarbons (PAHs; benzo[a]pyrene, benzo[k]fluoranthene, and benzo[ghi]perylene) that had log$K_{lip/w}$ between 7.0 and 7.6 but log$K_{BSA/w}$ only around 4.7. The equally hydrophobic flame retardants BDE-99, BDE-100 and BDE-153 fell much better on the MBM prediction due to the higher log$K_{BSA/w}$ (5.9-6.5; Table S2). The deviation was larger for the protein-dominated SH-SY5Y medium, which confirms that most likely the cellular protein binding of the PAHs was underestimated by log$K_{BSA/w}$.

IOCs, that is, partially or full charged organic acids and bases, showed an inconsistent picture (Figure 3C). After applying the speciation-corrected $D_{lip/w}$(pH 7.4) and $D_{BSA/w}$(pH 7.4) (Table S2), agreement between the MBM with predicted and experimental distribution ratios was excellent (ratio 0.3-1.2) for

the bases (diphenhydramine, propranolol, metoprolol, verapamil and venlafaxine; all positively charged at pH 7.4; the range of MAPE in 4 cell lines: 3.1-4.2%) and the multiprotic substances (the range of MAPE in 4 cell lines: 5.3-7.0%) including labetalol (53% cationic, 42 % zwitterionic). However, in case of organic acids, the predicted $IC_{10,baseline}$ were 7 to 1100 times higher for the experimental *D* values (Figure 3C; the range of MAPE in 4 cell lines: 109-105678%). The reason for this discrepancy is the high and specific binding affinity of organic acids to BSA that is much higher than predicted by eq. 12 as discussed above. We tentatively developed a simplified MBM model for organic acids based on experimental $D_{cell/w}$, $D_{medium/w}$ and $D_{SP/w}$, which is preliminary due to lack of sufficient number of data and described in Text S1 and Figure S3.

Simplifying the baseline MBM to an empirical QSAR. Based on the four bioassays, a generic model for baseline toxicity was established for the following assay condition: mammalian cells, FBS content of medium up to 10%, 24 h exposure in 384-well plate format (Figure 4). The generic assay condition was determined by averaging the volume fraction of proteins and lipids of the four cell lines ($Vf_{protein,cell}$ of 6% and $Vf_{lip,cell}$ of 1%) and assigning typical medium composition ($Vf_{protein,medium}$ of 0.3% and $Vf_{lip,medium}$ of 0.001%) and total volume of cells V_{cell} of 30 nL in 40 µL medium (V_{medium}). The determined volume fraction for the typical assay conditions were substituted into eq. 9 and expanded to IOCs by exchanging $K_{lip/w}$ with $D_{lip/w}$, yielding an equation with only one input parameter, $D_{lip/w}$(pH7.4) (eq. 18, "(pH 7.4)" omitted for simplicity).

$$IC_{10,baseline}(M)=6.9\times10^{-4}\times\left(1+\frac{93}{D_{lip/w}}+\frac{6\times10^{\left(0.72\ \log D_{lip/w}+0.34\right)}}{D_{lip/w}}\right)\times\left(7.5\times10^{-4}+\frac{0.003\times10^{\left(0.72\ \log D_{lip/w}+0.34\right)}+10^{-5}\ D_{lip/w}+0.99}{0.06\times\ 10^{\left(0.72\ \log D_{lip/w}+0.34\right)}+10^{-2}\ D_{lip/w}+0.93}\right) \quad (18)$$

Figure 4 compares the bioassay-specific simulations from Figure 3A with the simulations for a generic cell and a generic media (eq. 18). The lipid and protein content of the medium had a larger influence on the curve shape for more hydrophobic chemicals (Figure 4). The cell composition seems not to have a large influence on the model (simulation not shown).

Despite having only one input parameter, eq. 18 remains rather complex and can be simplified into an exponential fit equation (eq.19) for practical applications.

$$\log(1/IC_{10,baseline}(M))=a+b\times\left(1-e^{-c\ \log D_{lip/w}(pH7.4)}\right) \quad (19)$$

This model (eq. 19) with the fit parameters in Table 2 is visually indistinguishable from eq. 18 and can be used for predictions for cell lines, where no protein and lipid contents are available, and the medium has not been characterized under the condition given above. In the same way, the bioassay-specific MBM was also simplified into exponential fit equations using best-fit values (Table 2).

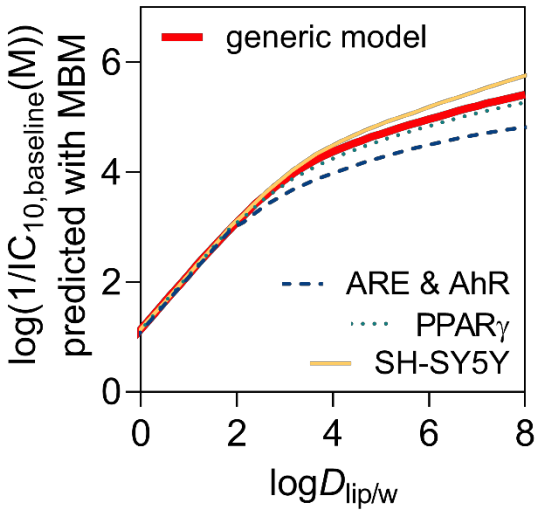

399

400 ***Figure 4. Simulation of hydrophobicity dependence of the MBM with CMB of 69 mM. Comparison of the***
401 ***bioassay-specific models (eq. 9 with eq. 12 as input) by specific cells and medium and a generic model (thick***
402 ***red line, eqs. 18 or 19; mammalian cells, FBS content of medium up to 10%, 24 h exposure in 384-well plate***
403 ***format).***

404 Despite partitioning processes being rather complex and different between neutral chemicals and IOCs,
405 there appears to be a common relationship between log$D_{lip/w}$(pH 7.4) and log(1/$IC_{10,baseline}$) independent
406 of the type of chemical and specific for each bioassay combination of cells and medium. Therefore, our
407 simplified model could be applied pragmatically as an "empirical QSAR" for anchoring the measured
408 effects in baseline toxicity. Although the relationship between $D_{lip/w}$(pH7.4) and $D_{BSA/w}$(pH7.4) was not
409 satisfied for organic acids (Figure 2B), even organic acids aligned with the predictions of the empirical
410 QSAR (eq. 19).

411

412 ***Table 2. Empirical QSAR for Baseline Toxicity: Best-fit Values from Exponential Fit Equation of Mass***
413 ***Balance Model (MBM) for Baseline Toxicity with Equation 19.***

Bioassay	Cells	Medium	Best-fit values (eq. 19)		
			a	b	c
generic[a]	generic cell	generic medium	1.23	4.97	0.236
AREc32	MCF7	DMEM Glutamax + 10 % FBS	1.25	4.01	0.281
AhR-CALUX	H4lle	DMEM Glutamax + 10 % FBS	1.25	4.02	0.28
PPARγ-BLA	HEK293H	OptiMEM + 2% FBS	1.27	4.71	0.241
SH-SY5Y	SH-SY5Y (differentiated)	Neurobasal medium	1.26	5.63	0.202

414 [a] Mammalian cells, FBS content of medium up to 10%, 24 h exposure in 384-well plate format

Deriving TR for classification. $IC_{10,baseline}$ was predicted using the bioassay-specific empirical QSAR for neutral and ionizable compounds, and was compared with experimentally determined IC_{10} to calculate TR (Figure 5). As our empirical QSAR entirely depends on $D_{lip/w}$(pH 7.4), more reliable $D_{lip/w}$(pH 7.4) would improve the confidence of our prediction. Due to the limited availability of experimental $D_{lip/w}$(pH 7.4), we took a weight-of-evidence approach to derive $D_{lip/w}$(pH 7.4), which means that experimental values were preferably used over predicted values (LSERD or K_{ow} QSAR) (Table S2). A challenge in our approach is that we cannot decide a priori if these chemicals act only as baseline toxicants. Therefore, we also had to take an iterative weight-of-evidence approach and calculate the toxic ratio for all chemicals and evaluate how many classify as baseline toxicants and if that would align with absence of a known specific mode of action. Likewise for those with a TR > 10 it was checked if they have a known specific mode of action.

A general observation can be made from Figure 5 that the more hydrophobic a chemical is, the more likely it is classified as baseline toxicant. Such an observation has been made even for reactive chemicals that are also hydrophobic,[48] suggesting that they might mainly act in the membrane, where they accumulate, rather than on their specific target site.

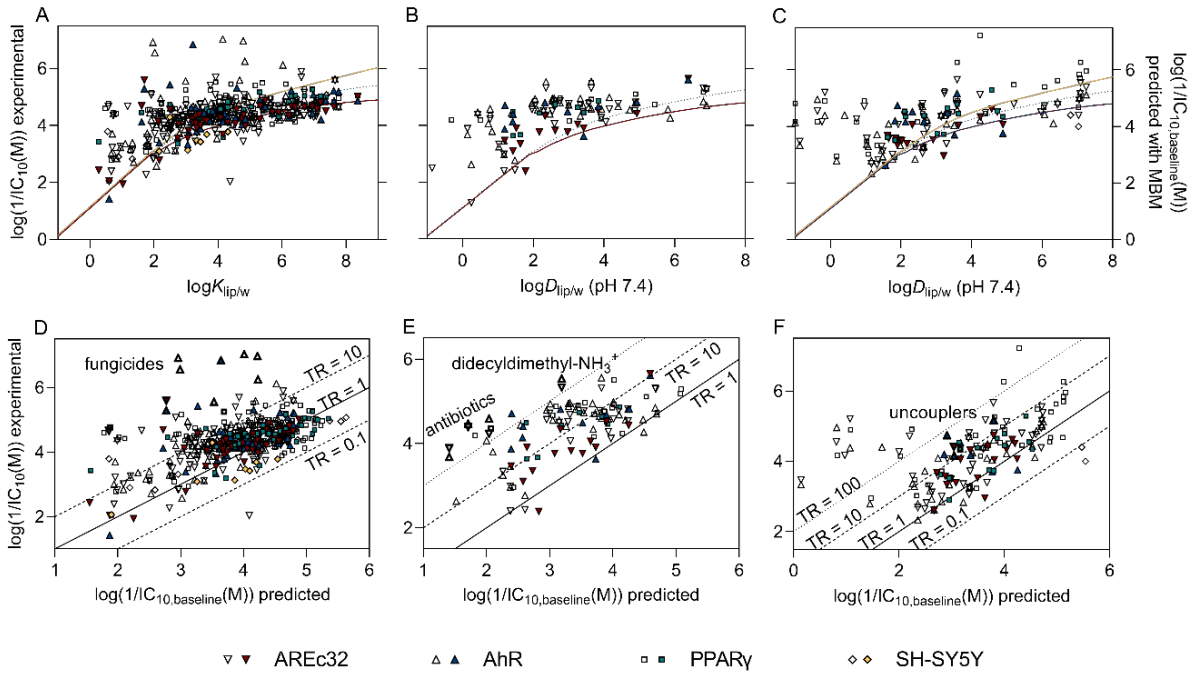

Figure 5. IC_{10} of (A) neutral, (B) cationic and multispecies, and (C) anionic chemicals as a function of experimental (filled symbols) and predicted (empty symbols) $D_{lip/w}$(pH 7.4) overlying the plot of the MBM prediction. Comparison of experimental IC_{10} with $IC_{10,baseline}$ for (D) neutral, (E) cationic and multispecies, and (F) anionic chemicals.

Classification of neutral compounds. Among 59 neutral chemicals with experimental $D_{lip/w}$(pH 7.4), experimental IC_{10} of 51 chemicals fell within a factor of 10 of the $IC_{10,baseline}$ prediction of the MBM and followed the bent baseline toxicity-hydrophobicity curve very well (Figure 5A). These 51 chemicals could be classified as baseline toxicants (TR < 10), while the remaining 8 chemicals indicated specific MOA with TR > 10 in one or more cell lines (Table S5). For further 194 chemicals with predicted $K_{lip/w}$, the majority also aligned well with the prediction of the MBM (Figure 5A). 88% (110/125) were baseline toxicants in AREc32, 79% (99/125) in AhR-CALUX, 80% (80/99) in PPARγ-BLA, and 83% (10/12) in SH-SY5Y (Figure 5D, Table S5). All 7 confirmed baseline toxicants by Vaes et al.[5] fell in the range of $0.1 < TR < 10$ either with predicted or experimental $D_{lip/w}$(pH 7.4), therefore, were successfully classified as baseline toxicants in all cell lines (experimental IC_{10} was only available for 6 baseline toxicants in PPARγ and SH-SY5Y) (Figure 5A).

19 neutral chemicals (4 chemicals with experimental and 15 with predicted $K_{lip/w}$) had a TR > 10 in AREc32, 32 (6 chemicals with experimental and 26 with predicted $K_{lip/w}$) in AhR-CALUX, 22 (3 chemicals with experimental and 19 with predicted $K_{lip/w}$) in PPARγ-BLA, and 2 (all with predicted $K_{lip/w}$) in SH-SY5Y (Figure 5D, Table S5). Many of those were just around 10, so the TR are quite uncertain given that the partition constant had been predicted. Therefore, we only had a closer look at 21 chemicals whose TR exceeded 50 at least in one cell line. Interestingly, fungicides including diverse strobilurins, dithianon, and isopyrazam were mainly affecting the AhR-CALUX, which could be potentially explained by differences in metabolic capacity of the three cell lines. Especially, strobilurin fungicides showed high TR in AhR-CALUX ranging from 562 to 9176, and they are inhibitors of the electron transport chain in mitochondria and are therefore potent general toxicants.[49, 50] In all three reporter gene cell lines, a cancer medicine etoposide showed high TRs between 230 and 271. The antimicrobial agent 1,2-benzisothiazolin-3-one had TRs between 25 and 95 and the fungicide octhilinone had TRs between 19 and 142 in all reporter gene cell lines. Some insecticides had rather high TRs in the reporter gene cell lines, but $D_{lip/w}$(pH 7.4) was predicted leading to uncertainty of the TR prediction. 3-Hydroxycarbofuran, a metabolite of the acetylcholinesterase inhibitor carbofuran, had a TR of 84 in SH-SY5Y and the fungicide azoxystrobin also had TR around 20 for SH-SY5Y. The observed specific toxicity of these chemicals could be aligned with their known mode of action.

Classification of IOCs. The IC_{10} of cationic and multispecies IOCs with experimental $D_{lip/w}$(pH 7.4) generally followed the trend of the empirical QSAR (Figure 5B, Table S6) but the TRs exceeded 10 for many bases and even 50 for a few bases, namely pindolol, irbesartan, and metoprolol (Figure 5E, Table

S6). A very large TR was predicted for some medicines including antibiotics and didecyldimethyl-ammonium but the $D_{lip/w}$(pH 7.4) for those were predicted and hence uncertain.

A similar picture was seen for the organic anions (Figure 5C, Table S6) with the majority following the empirical QSAR with exception of highly hydrophilic anionic chemicals, whose $D_{lip/w}$(pH 7.4) were predicted. Among the 25 organic acids with experimental $D_{lip/w}$(pH 7.4), 19 chemicals were baseline toxicants with TR < 10 and only 6 chemicals showed TR > 10 in one or more cell lines. Especially the substituted phenols (2,4-dinitrophenol, bromoxynil and dinoterb) had TR > 10 (Figure 5F), which is consistent with their specific mode of action of uncoupling. Many of the highly hydrophilic charged chemicals had TRs exceeding 100 but these results are uncertain because in all cases the $D_{lip/w}$(pH 7.4) were merely predicted and the empirical QSAR is uncertain at low $D_{lip/w}$(pH 7.4) values.

Two anionic compounds, hexachlorophene and 3,3',5,5'-tetrabromobisphenol A, were tested in SH-SY5Y and both showed TR even lower than 0.1 (Figure 5C, Table S6). This could be due to sorption of compounds to the plates, which was not considered in our prediction model. Larger sorption capacity to the well plastic can be observed especially in the medium with low content of lipids and proteins,[51] which is the case for SH-SY5Y. Furthermore, positively charged surface of collagen-coated plates could serve as a sink for anionic compounds in SH-SY5Y. The interaction with coating materials especially matters for SH-SY5Y as large area was uncovered with cells due to low number of cells used in the assay (Table 1), and collagen has positively charged amino acids at pH lower than 9.0.[52] Also, chemicals can be metabolized to less bioactive products, and IC_{10} of these chemicals will also be higher than $IC_{10,baseline}$ and hence may result in TR < 0.1.

CONCLUSION

The developed empirical QSAR would help to predict baseline toxicity of chemicals simply based on their hydrophobicity and is applicable even for chemicals without experimentally determined partition constants simply based on the K_{ow} but precision and accuracy increase when experimental partition ratios to cell lipids and proteins were used. This empirical QSAR is suitable for any type of chemicals including hydrophobic and ionizable chemicals but needs to be applied for organic acids with caution. The generic model derived from average of our assay condition provides a prediction tool that can be applied broadly to other bioassays having condition comparable to our assays.

Specificity of MOA can be quantified by comparing the actual toxicity of chemicals with predicted baseline toxicity from the empirical QSAR. The prediction of baseline toxicity also can provide the evidence to determine reasonable dosing concentration considering expected minimal toxicity level, not merely testing the same concentration over diverse compounds with different toxicity level.

ASSOCIATED CONTENT

Supporting Information

The Supporting Information is available free of charge on the ACS Publications website at doi:xxxxxx. Word file with more detailed information on the workflow and additional figures. Excel data table with compilation of physicochemical properties, cytotoxicity data and model results.

AUTHOR INFORMATION

Corresponding Author

*Phone: +49 341 235-1244. Fax: +49 341 235-1787. E-mail: beate.escher@ufz.de

ORCID

Beate Escher: 0000-0002-5304-706X

Jungeun Lee: 0000-0001-8336-2952

Funding

The robotic HTS systems and the D300 dispenser are a part of the major infrastructure initiative CITEPro (Chemicals in the Environment Profiler) funded by the Helmholtz Association with co-funding by the States of Saxony and Saxony-Anhalt.

Notes

The authors declare no competing financial interest.

ACKNOWLEDGMENTS

We thank Jenny Braasch, Andreas Baumer, and Niklas Wojtysiak for experimental assistance.

REFERENCES

(1) Verhaar, H. J. M., van Leeuwen, C. J., and Hermens, J. L. M. (1992) Classifying environmental pollutants. *Chemosphere 25*, 471-491.

(2) Escher, B. I., and Hermens, J. L. M. (2002) Modes of action in ecotoxicology: Their role in body burdens, species sensitivity, QSARs, and mixture effects. *Environ. Sci. Technol. 36*, 4201-4217.

(3) Maeder, V., Escher, B. I., Scheringer, M., and Hungerbuhler, K. (2004) Toxic ratio as an indicator of the intrinsic toxicity in the assessment of persistent, bioaccumulative, and toxic chemicals. *Environ. Sci. Technol. 38*, 3659-3666.

(4) Ramos, E. U., Vaes, W. H. J., Verhaar, H. J. M., and Hermens, J. L. M. (1998) Quantitative structure-activity relationships for the aquatic toxicity of polar and nonpolar narcotic pollutants. *J. Chem. Inf. Comput. Sci. 38*, 845-852.

(5) Vaes, W. H. J., Ramos, E. U., Verhaar, H. J. M., and Hermens, J. L. M. (1998) Acute toxicity of nonpolar versus polar narcosis: Is there a difference? *Environ. Toxicol. Chem. 17*, 1380-1384.

(6) Klüver, N., Vogs, C., Altenburger, R., Escher, B. I., and Scholz, S. (2016) Development of a general baseline toxicity QSAR model for the fish embryo acute toxicity test. *Chemosphere 164*, 164-173.

(7) Escher, B. I., Baumer, A., Bittermann, K., Henneberger, L., König, M., Kühnert, C., and Klüver, N. (2017) General baseline toxicity QSAR for nonpolar, polar and ionisable chemicals and their mixtures in the bioluminescence inhibition assay with *Aliivibrio fischeri*. *Environ. Sci. Process. Impacts 19*, 414-428.

(8) Klüver, N., Bittermann, K., and Escher, B. I. (2019) QSAR for baseline toxicity and classification of specific modes of action of ionizable chemicals in the zebrafish embryo toxicity test. *Aquat. Toxicol. 207*, 110-119.

(9) Escher, B. I., Glauch, L., Konig, M., Mayer, P., and Schlichting, R. (2019) Baseline Toxicity and Volatility Cutoff in Reporter Gene Assays Used for High-Throughput Screening. *Chem. Res. Toxicol. 32*, 1646-1655.

(10) Fischer, F., Henneberger, L., König, M., Bittermann, K., Linden, L., Goss, K.-U., and Escher, B. (2017) Modeling exposure in the Tox21 *in vitro* bioassays. *Chem. Res. Toxicol. 30*, 1197−1208.

(11) Proenca, S., Escher, B. I., Fischer, F. C., Fisher, C., Gregoire, S., Hewitt, N. J., Nicol, B., Paini, A., and Kramer, N. I. (2021) Effective exposure of chemicals in *in vitro* cell systems: A review of chemical distribution models. *Toxicol. In Vitro 73*, 105133.

(12) van Wezel, A., and Opperhuizen, A. (1995) Narcosis Due to Environmental-Pollutants in Aquatic Organisms - Residue-Based Toxicity, Mechanisms, and Membrane Burdens. *Crit. Rev. Toxicol. 25*, 255-279.

(13) Escher, B. I., Eggen, R. I. L., Schreiber, U., Schreiber, Z., Vye, E., Wisner, B., and Schwarzenbach, R. P. (2002) Baseline toxicity (narcosis) of organic chemicals determined by *in vitro* membrane potential measurements in energy-transducing membranes. *Environ. Sci. Technol. 36*, 1971-1979.

(14) Escher, B. I., Ashauer, R., Dyer, S., Hermens, J. L., Lee, J. H., Leslie, H. A., Mayer, P., Meador, J. P., and Warne, M. S. (2011) Crucial role of mechanisms and modes of toxic action for understanding tissue residue toxicity and internal effect concentrations of organic chemicals. *Integr Environ Assess Manag 7*, 28-49.

(15) Armitage, J. M., Wania, F., and Arnot, J. A. (2014) Application of Mass Balance Models and the Chemical Activity Concept To Facilitate the Use of in Vitro Toxicity Data for Risk Assessment. *Environ. Sci. Technol. 48*, 9770-9779.

(16) Henneberger, L., Mühlenbrink, M., Fischer, F. C., and Escher, B. I. (2019) C18-Coated Solid-Phase Microextraction Fibers for the Quantification of Partitioning of Organic Acids to Proteins, Lipids, and Cells. *Chem. Res. Toxicol. 32*, 168 - 178.
(17) Huchthausen, J., Mühlenbrink, M., Konig, M., Escher, B. I., and Henneberger, L. (2020) Experimental Exposure Assessment of Ionizable Organic Chemicals in *In Vitro* Cell-Based Bioassays. *Chem. Res. Toxicol. 33*, 1845-1854.
(18) Endo, S., Escher, B. I., and Goss, K. U. (2011) Capacities of Membrane Lipids to Accumulate Neutral Organic Chemicals. *Environ. Sci. Technol. 45*, 5912-5921.
(19) Endo, S., and Goss, K. U. (2011) Serum albumin binding of structurally diverse neutral organic compounds: data and models. *Chem. Res. Toxicol. 24*, 2293-2301.
(20) deBruyn, A. M. H., and Gobas, F. A. P. C. (2007) The sorptive capacity of animal protein. *Environ. Toxicol. Chem. 26*, 1803-1808.
(21) Gobas, F. A. P. C., Lahittete, J. M., Garofalo, G., Wan, Y. S., and Mackay, D. (1988) A novel method for measuring membrane-water partition coefficients of hydrophobic organic chemicals: comparison with 1-octanol-water partitioning. *J. Pharm. Sci. 77*, 265-272.
(22) US EPA. (2020) Chemistry Dashboard. https://comptox.epa.gov/dashboard/ accessed on 20 Dec 2020.
(23) ACD/Percepta. (2015) *Build 2726, Advanced Chemistry Development, Inc., Toronto, On, Canada, http://www.acdlabs.com*.
(24) Betageri, G. V., and Rogers, J. A. (1987) Thermodynamics of partitioning of beta-blockers in the normal-octanol-buffer and liposome systems. *Int. J. Pharm. 36*, 165-173.
(25) Vaes, W. H. J., Ramos, E. U., Hamwijk, C., vanHolsteijn, I., Blaauboer, B. J., Seinen, W., Verhaar, H. J. M., and Hermens, J. L. M. (1997) Solid phase microextraction as a tool to determine membrane/water partition coefficients and bioavailable concentrations in in vitro systems. *Chem. Res. Toxicol. 10*, 1067-1072.
(26) Avdeef, A., Box, K. J., Comer, J. E. A., Hibbert, C., and Tam, K. Y. (1998) pH-metric logP 10. Determination of liposomal membrane-water partition coefficients of ionizable drugs. *Pharm. Res. 15*, 209-215.
(27) Escher, B. I., Schwarzenbach, R. P., and Westall, J. C. (2000) Evaluation of liposome-water partitioning of organic acids and bases. 1. Development of a sorption model. *Environ. Sci. Technol. 34*, 3954-3961.
(28) Jabusch, T. W., and Swackhamer, D. L. (2005) Partitioning of polychlorinated biphenyls in octanol/water, triolein/water, and membrane/water systems. *Chemosphere 60*, 1270-1278.
(29) Kwon, J. H., Liljestrand, H. M., and Katz, L. E. (2006) Partitioning of moderately hydrophobic endocrine disruptors between water and synthetic membrane vesicles. *Environ. Toxicol. Chem. 25*, 1984-1992.
(30) Endo, S., Mewburn, B., and Escher, B. I. (2013) Liposome and protein-water partitioning of polybrominated diphenyl ethers (PBDEs). *Chemosphere 90*, 505-511.
(31) Quinn, C. L., van der Heijden, S. A., Wania, F., and Jonker, M. T. O. (2014) Partitioning of Polychlorinated Biphenyls into Human Cells and Adipose Tissues: Evaluation of Octanol, Triolein, and Liposomes as Surrogates. *Environ. Sci. Technol. 48*, 5920-5928.
(32) Ulrich, N., Endo, S., Brown, T. N., Watanabe, N., Bronner, G., Abraham, M. H., and Goss, K.-U. (2017) UFZ-LSER database v 3.2.1, Helmholtz Centre for Environmental Research-UFZ, Leipzig, Germany [accessed on 05.02.2021]; http://www.ufz.de/lserd.
(33) Bittermann, K., Spycher, S., Endo, S., Pohler, L., Huniar, U., Goss, K.-U., and Klamt, A. (2014) Prediction of Phospholipid-Water Partition Coefficients of Ionic Organic Chemicals Using the Mechanistic Model COSMOmic. *J. Phys. Chem. B 118*, 14833-14842.
(34) Ebert, A., Allendorf, F., Berger, U., Goss, K. U., and Ulrich, N. (2020) Membrane/Water Partitioning and Permeabilities of Perfluoroalkyl Acids and Four of their Alternatives and the Effects on Toxicokinetic Behavior. *Environ. Sci. Technol. 54*, 5051-5061.
(35) Henneberger, L., Mühlenbrink, M., Heinrich, D., Teixeira, A., Nicol, B., and Escher , B. I. (2020) Experimental Validation of Mass Balance Models for *in vitro* Cell-based Bioassays. *Environ. Sci. Technol. 54*, 1120-1127.

(36) Escher, B., Abagyan, R., M, E., Klüver, N., Redman, A., Zarfl, C., and Parkerton, T. (2020) Recommendations for improving methods and models for aquatic hazard assessment of ionizable organic chemicals. *Environ. Toxicol. Chem. 39*, 269-286.
(37) Vaes, W. H. J., Ramos, E. U., Verhaar, H. J. M., Seinen, W., and Hermens, J. L. M. (1997) Measurement of free concentrations using solid phase microextraction: binding to protein. *Anal. Chem. 68*, 4463-4467.
(38) Henneberger, L., Goss, K. U., and Endo, S. (2016) Equilibrium Sorption of Structurally Diverse Organic Ions to Bovine Serum Albumin. *Environ. Sci. Technol. 50*, 5119-5126.
(39) Allendorf, F., Berger, U., Goss, K. U., and Ulrich, N. (2019) Partition coefficients of four perfluoroalkyl acid alternatives between bovine serum albumin (BSA) and water in comparison to ten classical perfluoroalkyl acids. *Environ. Sci. Process. Impacts 21*, 1852-1863.
(40) Henneberger, L., Goss, K. U., and Endo, S. (2016) Partitioning of Organic Ions to Muscle Protein: Experimental Data, Modeling, and Implications for *in Vivo* Distribution of Organic Ions. *Environ. Sci. Technol. 50*, 7029-7036.
(41) Escher, B., Neale, P. A., and Villeneuve, D. (2018) The advantages of linear concentration-response curves for *in vitro* bioassays with environmental samples. *Environ. Toxicol. Chem. 37*, 2273–2280.
(42) Escher, B. I., van Daele, C., Dutt, M., Tang, J. Y. M., and Altenburger, R. (2013) Most oxidative stress response in water samples comes from unknown chemicals: the need for effect-based water quality trigger values. *Environ. Sci. Technol. 47*, 7002-7011.
(43) Neale, P. A., Altenburger, R., Ait-Aissa, S., Brion, F., Busch, W., de Aragão Umbuzeiro, G., Denison, M. S., Du Pasquier, D., Hilscherova, K., Hollert, H., Morales, D. A., Novac, J., Schlichting, R., Seiler, T.-B., Serra, H., Shao, Y., Tindall, A. J., Tollefsen, K. E., Williams, T. D., and Escher, B. I. (2017) Development of a bioanalytical test battery for water quality monitoring: Fingerprinting identified micropollutants and their contribution to effects in surface water. *Water Res. 123*, 734-750.
(44) Escher, B. I., Henneberger, L., Schlichting, R., and Fischer, F. C. (2020) Cytotoxicity burst or baseline toxicity? Differentiating specific from nonspecific effects in reporter gene assays. *Environ. Health Perspect. 128*, 077007.
(45) Neale, P. A., Braun, G., Brack, W., Carmona, E., Gunold, R., Konig, M., Krauss, M., Liebmann, L., Liess, M., Link, M., Schafer, R. B., Schlichting, R., Schreiner, V. C., Schulze, T., Vormeier, P., Weisner, O., and Escher, B. I. (2020) Assessing the Mixture Effects in *In Vitro* Bioassays of Chemicals Occurring in Small Agricultural Streams during Rain Events. *Environ. Sci. Technol. 54*, 8280-8290.
(46) Escher, B. I., and Neale, P. A. (2021) Effect-based trigger values for mixtures of chemicals in surface water detected with *in vitro* bioassays. *Environ. Toxicol. Chem. 40*, 487-499.
(47) Endo, S., Brown, T. N., and Goss, K.-U. (2013) General model for estimating partition coefficients to organisms and their tissues using the biological compositions and polyparameter Linear Free Energy Relationships. *Environ. Sci. Technol. 47*, 6630−6639.
(48) Freidig, A. P., Verhaar, H. J. M., and Hermens, J. L. M. (1999) Comparing the potency of chemicals with multiple modes of action in aquatic toxicology: Acute toxicity due to narcosis versus reactive toxicity of acrylic compounds. *Environ. Sci. Technol. 33*, 3038-3043.
(49) Mansfield, R. W., and Wiggins, T. E. (1990) Photoaffinity labelling of the β-methoxyacrylate binding site in bovine heart mitochondrial cytochrome bc1 complex. *Biochim. Biophys. Acta. Bioenerg. 1015*, 109-115.
(50) Müller, M. E., Vikstrom, S., König, M., Schlichting, R., Zarfl, C., Zwiener, C., and Escher , B. I. (2019) Mitochondrial toxicity of micropollutants in water samples measured by the oxygen consumption rate in cells. *Environ. Toxicol. Chem. 38*, 1000–1011.
(51) Fischer, F. C., Cirpka, O. A., Goss, K. U., Henneberger, L., and Escher, B. I. (2018) Application of Experimental Polystyrene Partition Constants and Diffusion Coefficients to Predict the Sorption of Neutral Organic Chemicals to Multiwell Plates in *in Vivo* and *in Vitro* Bioassays. *Environ. Sci. Technol. 52*, 13511-13522.
(52) Uquillas, J. A., and Akkus, O. (2012) Modeling the Electromobility of Type-I Collagen Molecules in the Electrochemical Fabrication of Dense and Aligned Tissue Constructs. *Ann. Biomed. Eng. 40*, 1641-1653.

690